PCCP

Cite this: *Phys. Chem. Chem. Phys.*, 2012, **14**, 575–588

www.rsc.org/pccp

PAPER

Crossed beam reactions of methylidyne [$CH(X^2\Pi)$] with D2-acetylene [$C_2D_2(X^1\Sigma_g^+)$] and of D1-methylidyne [$CD(X^2\Pi)$] with acetylene [$C_2H_2(X^1\Sigma_g^+)$]

Ralf I. Kaiser,* Xibin Gu, Fangtong Zhang and Pavlo Maksyutenko

Received 17th August 2011, Accepted 19th October 2011
DOI: 10.1039/c1cp22635e

The crossed molecular beam reactions of ground state methylidyne, $CH(X^2\Pi)$, with D2-acetylene, $C_2D_2(X^1\Sigma_g^+)$, and of D1-methylidyne, $CD(X^2\Pi)$, with acetylene, $C_2H_2(X^1\Sigma_g^+)$, were conducted under single collision conditions at a collision energy of 17 kJ mol^{-1}. Four competing reaction channels were identified in each system following atomic 'hydrogen' (H/D) and molecular 'hydrogen' ($H_2/D_2/HD$) losses. The reaction dynamics were found to be indirect *via* complex formation and were initiated by two barrierless-addition pathways of methylidyne/D1-methylidyne to one and to both carbon atoms of the D2-acetylene/acetylene reactant yielding HCCDCD/DCCHCH and c-C_3D_2H/c-C_3H_2D collision complexes, respectively. The latter decomposed *via* atomic hydrogen/deuterium ejection to form the thermodynamically most stable cyclopropenylidene species (c-C_3H_2, c-C_3D_2, c-C_3DH). On the other hand, the HCCDCD/DCCHCH adducts underwent hydrogen/deuterium shifts to form the propargyl radicals (HDCCCD, D_2CCCH; HDCCCH, H_2CCCD) followed by molecular 'hydrogen' losses within the rotational plane of the decomposing complex yielding l-C_3H/l-C_3D. Quantitatively, our crossed beam studies suggest a dominating atomic compared to molecular 'hydrogen' loss with fractions of 81 ± 23% *vs.* 19 ± 10% for the CD/C_2H_2 and 87 ± 30% *vs.* 13 ± 4% for the CH/C_2D_2 systems. The role of these reactions in the formation of interstellar isomers of C_3H_2 and C_3H is also discussed.

1. Introduction

Resonantly stabilized free radicals (RSFRs) are crucial reaction intermediates involved in the formation of polycyclic aromatic hydrocarbons (PAHs)[1–15] together with their hydrogen deficient precursors of soot particles in combustion processes.[9,16–19] The propargyl radical (C_3H_3; X^2B_1) is considered as a prototype RSFR, in which the unpaired electron is delocalized and spread out over two or more sites in the molecule. This results in a number of resonant electronic structures of comparable importance such as the 'acetylenic' ($H_2C–C\equiv CH$) and 'allenic' ($H_2C=C=CH$) resonant forms.[20–22] The self-reaction of the propargyl radical is suggested to present one of the most significant cyclization steps in flames of aliphatic fuels ultimately forming benzene which decomposes to the phenyl radical plus a hydrogen atom.[23–33]

Since the propargyl radical represents the prototype of a RSFR, its stability and unimolecular decomposition have been studied extensively to date.[26,29,31,34–46] A recent overview was disseminated by Maksyutenko *et al.* in this journal.[47] Briefly, the unimolecular decomposition of propargyl[48] has been suggested to form predominantly C_3H_2 isomers cyclopropenylidene (c-C_3H_2; X^1A_1), propargylene (HCCCH; X^3B), and vinylidene carbene (H_2CCC; X^1A_1).[30,49–60] These isomers present also important building blocks in the formation of PAHs and related molecules due to the equilibrium reactions with hydrogen atoms, which access the C_3H_3 surface *via* the generic reaction $C_3H_2 + H \leftrightarrow C_3H_3$.[61–66] The synthesis of C_3H_2 isomers was also studied experimentally and theoretically by investigating the unimolecular decomposition of chemically activated C_3H_3 molecules formed in the reaction of methylidyne radicals, $CH(X^2\Pi)$, with acetylene, $C_2H_2(X^1\Sigma_g^+)$, and of ground state carbon atoms, $C(^3P_j)$, with the vinyl radical, C_2H_3 (X^2A').[67,68] Experimentally, the unimolecular decomposition of C_3H_3 radicals can also be studied under molecular beam conditions *via* photodissociation of the propargyl radical. Photodissociation of the propargyl radical in the range of 242 to 248 nm[69] suggested that electronic excitation was followed by internal conversion to the ground state surface followed by a statistical decay to the products. The authors concluded that the most likely product was cyclopropenylidene (c-C_3H_2). Photodissociation studies of isotopically substituted propargyl (D_2CCCH) radicals showed complete isotopic scrambling. The authors proposed a unimolecular decomposition of a C_3H_2D intermediate formed *via* an internal [1,2] hydrogen

Department of Chemistry, University of Hawaii at Manoa, Honolulu, HI 96822, USA

shift followed by cyclization. Also, Butler *et al.*[70] examined the unimolecular dissociation of propargyl (C_3H_3) indicating that H_2CCC is preferentially contributing on the fast side of the time-of-flight (TOF) distribution; c-C_3H_2 is likely the dominant isomer formed in the dissociation of propargyl radicals with energies near the dissociation threshold. A photodissociation study of propargyl at 248 nm by Neumark *et al.*[71] suggested the propargyl radical fragmented *via* atomic and molecular hydrogen loss with propargylene (HCCCH) being dominant.[71] A computational study of propargyl photodissociation at 193 and 242 nm by Mebel *et al.*[72] verifies the overall branching ratio of the atomic *versus* molecular hydrogen loss (97%/3%) measured by Neumark *et al.* at 242 nm.

Besides theoretical and photodissociation studies, the reaction of methylidyne radicals with acetylene was also investigated in kinetics studies implying a barrier-less addition of methylidyne to the acetylene molecule down to 23 K.[67,73,74] Isothermal discharge flow reactor studies indicated that for an elevated temperature of 600 K and 2 Torr, atomic and molecular hydrogen pathways lead to C_3H_2 and C_3H isomers of about 85% and 15%, respectively.[75] On the other hand, employing the detection of hydrogen atoms *via* laser induced fluorescence (LIF), McKee *et al.* proposed an almost exclusive formation of C_3H_2 isomers of unknown structure.[76] Loison and Bergeat reported in a low-pressure fast flow reactor study that the hydrogen atom loss channel contributed to only 90%.[68] The most recent kinetics study by Goulay *et al.*[77] revealed the formation of the cyclic and C_2 symmetric C_3H_2 isomers. The only experimental investigation of the methylidyne–acetylene system under single collision conditions was conducted utilizing the crossed molecular beams approach. Maksyutenko *et al.* provided evidence that at a collision energy of 16.8 kJ mol^{-1}, both the atomic and molecular hydrogen loss pathways forming C_3H_2 and l-C_3H isomers, respectively, were open with fractions of about 91 ± 10% and 9 ± 2%, respectively. Considering the C_3H_2 isomers, energetical constraints indicate that the thermodynamically most stable c-C_3H_2 isomer was formed;[47] within the constraints of a two channel fit, the formation of c-C_3H_2 (31.5 ± 5.0%) and $HCCCH/H_2CCC$ (59.5 ± 5.0%) could fit the data as well.

In this paper, we expand these investigations under single collision conditions and present results of the crossed beam reactions of methylidyne, CH($X^2\Pi$), with D2-acetylene, $C_2D_2(X^1\Sigma_g^+)$, and of D1-methylidyne, CD($X^2\Pi$), with acetylene, $C_2H_2(X^1\Sigma_g^+)$. These studies are aimed to 'trace' the incorporation of the hydrogen *versus* deuterium atom and probe the formation of atomic hydrogen and deuterium *versus* the molecular 'hydrogen' elimination pathway leading to HD, H_2, and D_2. These data are then discussed within the context of previous experimental and theoretical studies of this system to gain a more complete understanding of the reaction of methylidyne radicals with acetylene together with their partially deuterated counterparts and of the role of distinct $C_3H_3/C_3H_2D/C_3D_2H$ isotopomers/isotopologues in the underlying reaction dynamics.

2. Experimental

The crossed beam reactions of methylidyne, CH($X^2\Pi$), with D2-acetylene, $C_2D_2(X^1\Sigma_g^+)$, and of D1-methylidyne, CD($X^2\Pi$), with acetylene, $C_2H_2(X^1\Sigma_g^+)$, were carried out in a universal crossed molecular beams machine under single collision conditions.[47,78–82] Briefly, pulsed supersonic beams of ground state methylidyne, CH($X^2\Pi$), and D1-methylidyne, CD($X^2\Pi$), were generated *via* photolysis of helium-seeded bromoform ($CHBr_3$) (Sigma Aldrich, ≥ 99%) and D1-bromoform ($CDBr_3$) (Sigma Aldrich, 99.5% D), respectively. Helium gas (99.9999%; Gaspro) at a pressure of 2.2 atm was bubbled through a stainless steel container, which acted as a reservoir for the bromoform and D1-bromoform samples held at a temperature of 283 K. This resulted in seeding fractions of 0.12% bromoform and D1-bromoform in helium. The mixtures were fed into a pulsed piezoelectric valve operated at a repetition rate of 60 Hz, pulse widths of 80 μs, and a peak voltage of −400 to −450 V. The output of an excimer laser (KrF, 248 nm, 60 mJ per pulse) was focused downstream of the nozzle to an area of about 4.0 mm by 0.7 mm. Number densities of a few 10^{12} radicals cm^{-3} can be formed in the interaction region of the scattering chamber.[82] The pulsed beam of the (D1)-methylidyne radicals passed through a skimmer, and a four-slit chopper wheel selected a part of this beam with a well-defined velocity (Table 1). This section of the pulse was timed to intercept the most intense section of a pulsed acetylene or D2-acetylene beam perpendicularly in the interaction region of the scattering chamber. The peak velocities (v_p) and speed ratios (S) of the segments of the interacting beams together with the corresponding collision energies and center-of-mass angles are compiled in Table 1. Rotational and vibrational modes of the methylidyne radicals were characterized *via* laser induced fluorescence.[82] The beams were defined by typical rotational temperatures of 14 ± 1 K; the relative populations of the first vibrationally excited level ($\nu = 1$) was determined to be less than 6%. It is important to outline that the photodissociation of bromoform produces apart from methylidyne radical reactive species $CHBr_2$, CHBr, and CBr. However, when crossing with the secondary beam, these systems have considerably *lower* center-of-mass angles much closer to the primary beam due to the heavy bromine atom(s) in these fragments. We have shown previously for the methylidyne–acetylene system that the dynamics of bromine-containing radicals can be distinguished from those of the methylidyne reactions based on the distinct scattering angular ranges of the products.[47,82]

Table 1 Primary and secondary beam peak velocities (v_p), speed ratios (S), collision energies (E_c), and center-of-mass angles (Θ_{CM})

	v_p/ms^{-1}	S	E_c/kJ mol^{-1}	Θ_{CM}
CD($X^2\Pi$)	1720 ± 10	15 ± 1	17.2 ± 0.1	44.2 ± 0.2
$C_2H_2(X^1\Sigma_g^+)$	902 ± 2	16 ± 1		
CH($X^2\Pi$)	1730 ± 44	16 ± 1	16.8 ± 0.7	47.9 ± 0.8
$C_2D_2(X^1\Sigma_g^+)$	890 ± 5	15 ± 1		

Reactively scattered species were mass-filtered using a quadrupole mass spectrometric detector in the time-of-flight (TOF) mode after electron-impact ionization of the neutral molecules at 80 eV electron energy. The detector can be rotated within the plane defined by the primary and the secondary reactant beams to allow taking angular resolved TOF spectra. At each angle, up to 400 000 TOF spectra were accumulated. TOF spectra were

then integrated and normalized to extract the product angular distribution in the laboratory frame (LAB). In order to acquire information on the scattering dynamics, the laboratory data were transformed into the center-of-mass reference frame utilizing a forward-convolution routine.[83,84] This iterative method employs a parametrized or point-form angular flux distribution, $T(\theta)$, and a translational energy flux distribution, $P(E_T)$, in the center-of-mass system (CM). Laboratory TOF spectra and the laboratory angular distributions (LAB) are calculated from the $T(\theta)$ and $P(E_T)$ functions and are averaged over a grid of Newton diagrams accounting for the apparatus functions, beam divergences, and velocity spreads.

3. Results

3.1. CD/C_2H_2 System

We recorded scattering signals for the reaction of D1-methylidyne with acetylene at mass-to-charge ratios (m/z) of 39, 38, and 37; the time-of-flight (TOF) spectra and the corresponding laboratory angular distributions are shown in Fig. 1 and 2, respectively. First, a signal at m/z = 39 had to be fit with two contributions: reactive scattering signal from the atomic hydrogen (1 amu) loss channel forming C_3DH (39 amu) and non-reactively scattered $^{79}Br^{++}$. Note that atomic bromine, which is present in the primary beam, has two isotopes, ^{79}Br and ^{81}Br. Their doubly ionized species give rise to signals at m/z = 39.5 and 40.5, respectively. Our mass spectrometer was operated at a resolution of 1 amu to discriminate, for instance, the signal at m/z = 39 from m/z = 38 and m/z = 38 from 37. These settings allowed that non-reactively scattered, doubly ionized ^{79}Br (m/z = 39.5) leaks into m/z = 39. An operation of the mass spectrometer at a resolution of 0.5 amu, which would have avoided this issue, was impractical as the reactive scattering signal in the range from 39 to 37 amu at a resolution of 0.5 amu was found to diminish beyond an acceptable intensity. At a resolution of 1 amu, a non-reactively scattered signal was only observed at angles less than about 36° with a decaying intensity as the angle increases away from the primary beam; reactive scattering at m/z = 39 was spread from 20° to at least 62° within the scattering plane defined by both beams. The reactive scattering signal at m/z = 39 could be fit with a single channel, *i.e.* a center-of-mass translational energy distribution, $P(E_T)$, in point form and a parametrized center-of-mass angular distribution ($T(\theta)$). Second, the TOF spectra and LAB distribution of m/z = 38—after scaling—do not coincide with laboratory data obtained at m/z = 39. As a matter of fact, the signal at m/z = 38 had to be fit with three contributions: (i) dissociative ionization of C_3DH (39 amu) to C_3D^+ (38 amu), (ii) reactive scattering signal for the atomic deuterium loss channel C_3H_2 (38 amu) + D (2 amu), and (iii) reactive scattering signal for the molecular hydrogen elimination channel C_3D (38 amu) + H_2 (2 amu). Based on the laboratory data (TOF, LAB), it is obvious that a non-reactively scattered signal was not present at m/z = 38. Third, we would like to discuss the laboratory data collected at m/z = 37. Here, TOF and LAB distributions had to be fit with four pathways: (i) dissociative ionization of C_3DH (39 amu) yielding C_3H^+ (37 amu), (ii) dissociative ionization of C_3H_2 (38 amu) yielding C_3H^+ (37 amu), (iii) a reactive channel *via* HD elimination leading to C_3H (37 amu) + HD (3 amu), and (iv) a reactive channel originating from the reaction of ground state carbon atoms, present in the beam, with acetylene forming C_3H (37 amu) + H (1 amu).[38] The ground state carbon atoms are formed from photodissociation of a fraction of the methylidyne

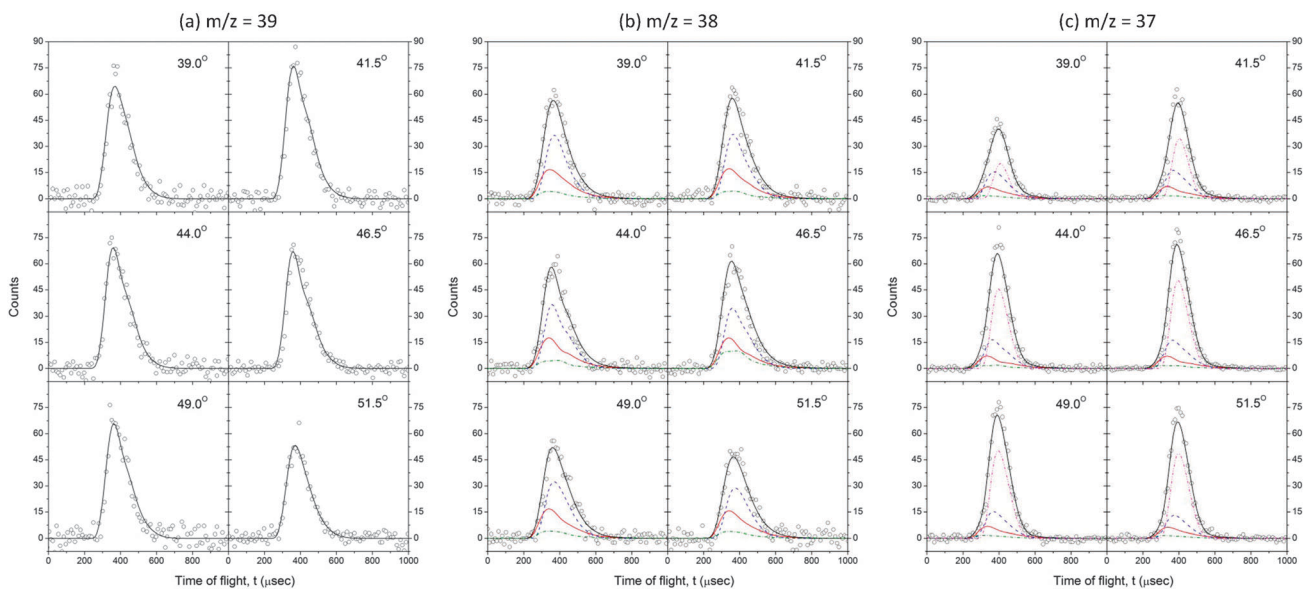

Fig. 1 Time-of-flight spectra collected during the reaction of D1-methylidyne radicals (CD) with acetylene (C_2H_2) at m/z = 39 (C_3HD^+) (a), m/z = 38 (b) (red solid: $C_3H_2^+$, blue dashed: C_3D^+ from dissociative electron impact ionization of C_3HD, olive dashed dotted: C_3D^+ from the molecular hydrogen loss channel, and m/z = 37, (c) (red solid: C_3H^+ from dissociative electron impact ionization of C_3H_2; blue dashed: C_3H^+ from dissociative electron impact ionization of C_3HD; olive dashed dotted: C_3D^+ from the HD loss channel; magenta dashed dotted: C_3H^+ from the reaction of carbon atoms with acetylene). The open circles represent the experimental data and the black solid lines represent the fits summing the contributions of the individual channels. Contributions from non-reactively scattered doubly ionized bromine have been subtracted.

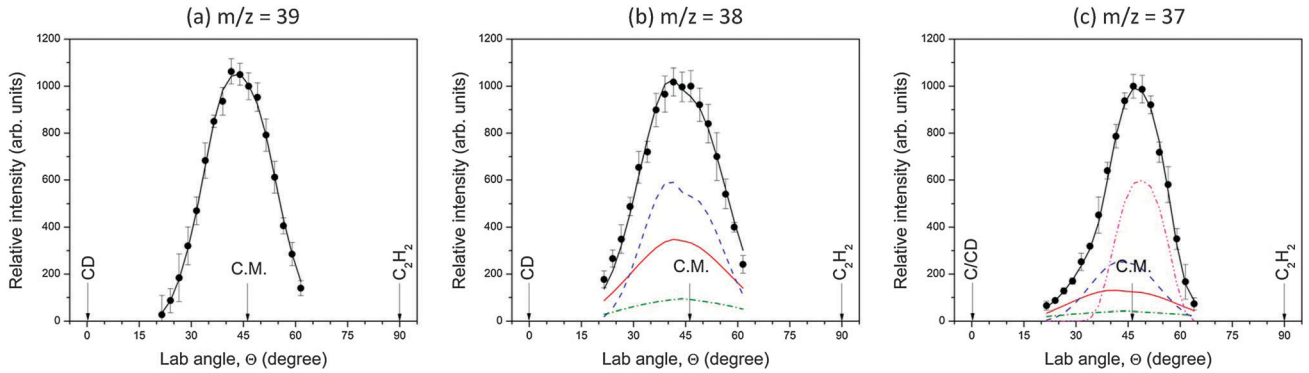

Fig. 2 Corresponding laboratory angular distributions of scattering signal recorded at m/z = 39, 38, and 37. The color codes are identical to those in the TOFs shown in Fig. 1. C.M. indicates the center-of-mass angle. Contributions from non-reactively scattered doubly ionized bromine have been subtracted.

radicals as demonstrated earlier.[47] However, since the reaction dynamics of this system were studied in our group over a broad range of collision energies from 8 to 31 kJ mol^{-1},[38] the incorporation of this reaction channel does not present a complication. To summarize, our laboratory data suggest that the reaction of D1-methylidyne radicals with acetylene involves four reactive scattering channels (1a)–(1d). Following the procedure as outlined in ref. 38, 83, and 84, we also extracted the branching ratios of the products formed under single collision conditions as stated in the square parentheses. The errors are derived from two factors: the experimental errors in the laboratory angular distributions, which translate to an uncertainty in the relative importance of two competing channels, and also the total ionization cross sections of the C_3H and the C_3 products.

$$\begin{aligned} CD + C_2H_2 &\rightarrow C_3DH + H \quad (1a) \quad [50 \pm 15\%] \\ &\rightarrow C_3H_2 + D \quad (1b) \quad [31 \pm 8\%] \\ &\rightarrow C_3D + H_2 \quad (1c) \quad [5 \pm 2\%] \\ &\rightarrow C_3H + HD \quad (1d) \quad [14 \pm 8\%] \end{aligned}$$

3.2. CH/C_2D_2 System

For the methylidyne–D2-acetylene system, data were collected from m/z = 40 to m/z = 37; the time-of-flight (TOF) spectra and the corresponding laboratory angular distributions are compiled in Fig. 3 and 4, respectively. First, the laboratory data at m/z = 40 could only be fit with two contributions, *i.e.* a reactive and non-reactive pathway: reactive scattering signal from the atomic hydrogen (1 amu) loss channel forming C_3D_2 (40 amu) and non-reactively scattered $^{81}Br^{++}$. Here, doubly ionized ^{81}Br yields signal at m/z = 40.5 which—at a resolution of 1 amu—leaks into 40 amu (*cf.* Section 3.1.). Second, at m/z = 39, two channels were necessary to reach an acceptable fit: a reactive scattering signal from the atomic deuterium (2 amu) loss channel forming C_3DH (39 amu) and non-reactively scattered $^{79}Br^{++}$. Third, the signal at m/z = 38 is very complex; four channels were necessary to fit the data: (i) dissociative electron impact ionization of the C_3D_2 (40 amu) product to give C_3D^+, (ii) dissociative electron impact ionization of the C_3DH (39 amu) product to C_3D^+, (iii) the reactive scattering channel from methylidyne plus D2-acetylene forming C_3D (38 amu) plus HD (3 amu), and (iv) a reactive channel originating from the reaction of ground state carbon atoms with D2-acetylene forming C_3D (38 amu) + D (2 amu).[38] Considering the first two channels, the dissociative electron impact ionization of neutral molecules leads to the formation of lower-mass fragments. In the present case, dissociative ionization of C_3D_2 (40 amu) and C_3DH (39 amu) can lead *via* ejection of a deuterium and hydrogen atom in both cases to C_3D^+, *i.e.* an ion with the mass-to-charge ratio of m/z = 38. The third channel presents a reactive scattering pathway which is formally equivalent to the emission of molecular hydrogen in the methylidyne–acetylene system studied earlier in our group.[38] Finally, in the case of channel four, the ground state carbon atoms are formed once again from photodissociation of a fraction of the methylidyne radicals as seen in the D1-methylidyne–acetylene reaction. However, since the reaction dynamics of the carbon atom–D2-acetylene system were studied in our group over a broad range of collision energies from 8 to 31 kJ mol^{-1},[38] the center-of-mass functions of this reaction channel are already known and do not present a complication. Finally, we were able to fit the laboratory data at m/z = 37 with two channels: (i) dissociative electron impact ionization of the C_3DH (39 amu) product to C_3H^+, and (ii) the reactive channel from methylidyne plus D2-acetylene forming C_3H (37 amu) plus D_2 (4 amu).

To summarize, our laboratory data indicate that the reaction of methylidyne radicals with D2-acetylene opens four reactive scattering channels (2a)–(2d) with the branching ratios of the products formed denoted in square parentheses.

$$\begin{aligned} CH + C_2D_2 &\rightarrow C_3D_2 + H \quad (2a) \quad [34 \pm 15\%] \\ &\rightarrow C_3DH + D \quad (2b) \quad [53 \pm 15\%] \\ &\rightarrow C_3D + HD \quad (2c) \quad [7 \pm 2\%] \\ &\rightarrow C_3H + D_2 \quad (2d) \quad [6 \pm 2\%] \end{aligned}$$

4. Discussion

To elucidate the reaction mechanisms involved and to propose the underlying dynamics, we are interpreting now the derived center of mass functions as compiled in Fig. 5 and 6 for the D1-methylidyne–acetylene and methylidyne–D2-acetylene systems, respectively. It should be highlighted that only those functions

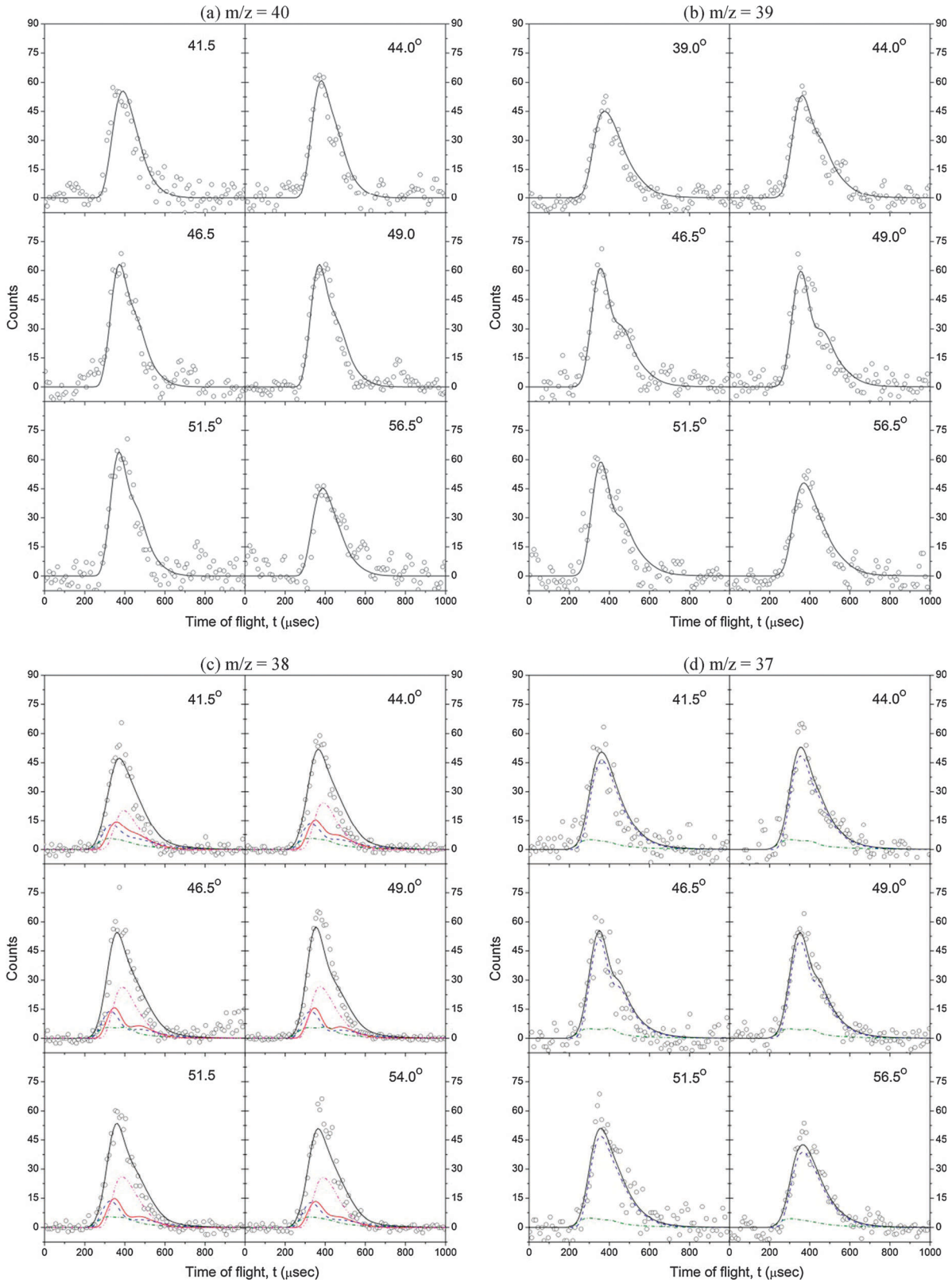

Fig. 3 Time-of-flight spectra collected during the reaction of methylidyne radicals (CH) with D2-acetylene (C_2D_2) recorded at $m/z = 40$ (a) ($C_3D_2^+$), $m/z = 39$ (b) (C_3HD^+), $m/z = 38$ (c) red solid: C_3D^+ from dissociative electron impact ionization of C_3D_2; blue dashed: C_3D^+ from dissociative electron impact ionization of C_3HD; olive dashed dotted: C_3D^+ from HD loss; magenta dashed dotted: C_3D^+ reaction of carbon atoms with D2-acetylene, and $m/z = 37$ (d) (blue dashed: C_3H^+ from dissociative electron impact ionization of C_3HD; olive dashed dotted: C_3H^+ from molecular deuterium loss channel). The open circles represent the experimental data and the black solid lines represent the fits summing the contributions of the individual channels. Contributions from non-reactively scattered doubly ionized bromine have been subtracted.

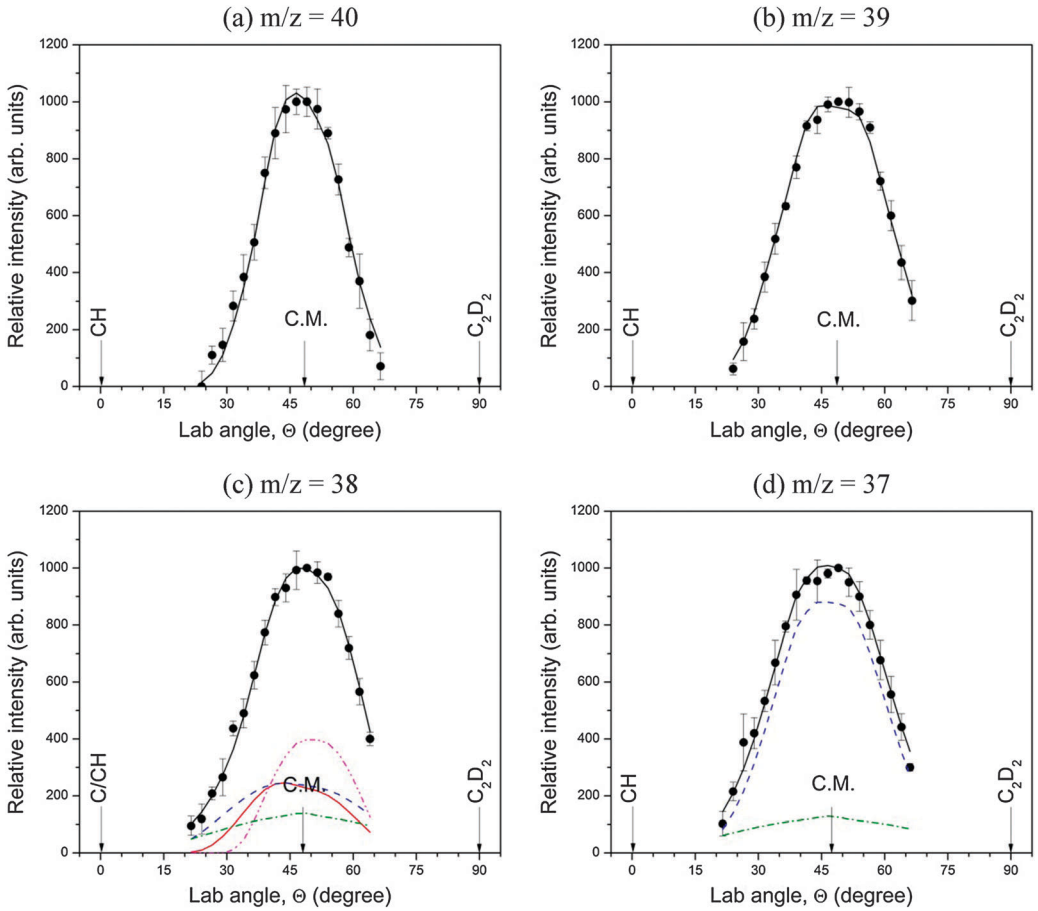

Fig. 4 Corresponding laboratory angular distributions of scattering signal recorded at m/z = 40, 39, 38, and 37. The color codes are identical to those in the TOFs as shown in Fig. 3. C.M. indicates the center-of-mass angle. Contributions from non-reactively scattered doubly ionized bromine have been subtracted.

relevant to the reaction of methylidyne radicals with acetylene are discussed; the dynamics of the atomic carbon–acetylene/D2-acetylene system, whose center-of-mass functions were necessary to fit data at m/z = 38 and 37, were published previously and the interested reader is referred to the relevant literature.[85]

4.1. CD/C_2H_2 System

Let us investigate the center-of-mass functions for the D1-methylidyne–acetylene reaction first. It is important to stress that the laboratory data for channels (1a) and (1b), *i.e.* the atomic hydrogen and deuterium loss pathways leading to C_3DH and C_3H_2, respectively, could be fit with essentially identical center-of-mass functions (Fig. 5). Here, the center-of-mass translational energy distribution for channels (1a) and (1b) extends to a maximum translational energy of 90–120 kJ mol^{-1}. Recall that for those molecules born with no internal excitation, the maximum translational energy allowed presents the arithmetic sum of the collision energy and the absolute of the reaction exoergicity. Therefore, a subtraction of the collision energy suggests a reaction exoergicity for channels (1a) and (1b) of 88 ± 15 kJ mol^{-1}. A comparison of this data with theoretically predicted energetics (Fig. 7) suggests that the thermodynamically most stable c-C_3DH and c-C_3H_2 isomers are formed. The best fit function of the center-of-mass angular distribution shows intensity over the complete angular range from 0° to 180° suggesting that the reaction dynamics are indirect and proceed *via* C_3H_2D complex(es). Further, best fits were achieved with slightly forward peaking functions, but within the error limits, a forward–backward distribution could also fit the data for channels (1a) and (1b). It should be highlighted that these center-of-mass functions for channels (1a) and (1b) are basically identical to the one derived for the C_3H_2 + H channel for the reaction of methylidyne radicals with acetylene.[47]

Similar to the atomic hydrogen/deuterium channels (1a) and (1b), indistinguishable center-of-mass functions could also be used to fit the laboratory data for the H_2 and HD elimination pathways leading to C_3D and C_3H, respectively. The reaction energy as extracted from the center-of-mass translational energy distribution is −93 ± 10 kJ mol^{-1} and correlates nicely with the theoretically predicted one of −103 kJ mol^{-1} to form l-C_3D and l-C_3H. The pronounced distribution maxima at about 30 kJ mol^{-1} suggest relatively tight exit transition states upon the H_2 and HD losses and hence a reorganization of the electron density from the reaction intermediate to the final products. Considering the center-of-mass angular distribution, the forward–backward symmetry and intensity over the complete angular range from 0° to 180° propose indirect scattering dynamics and a life time of the decomposing C_3H_2D complex

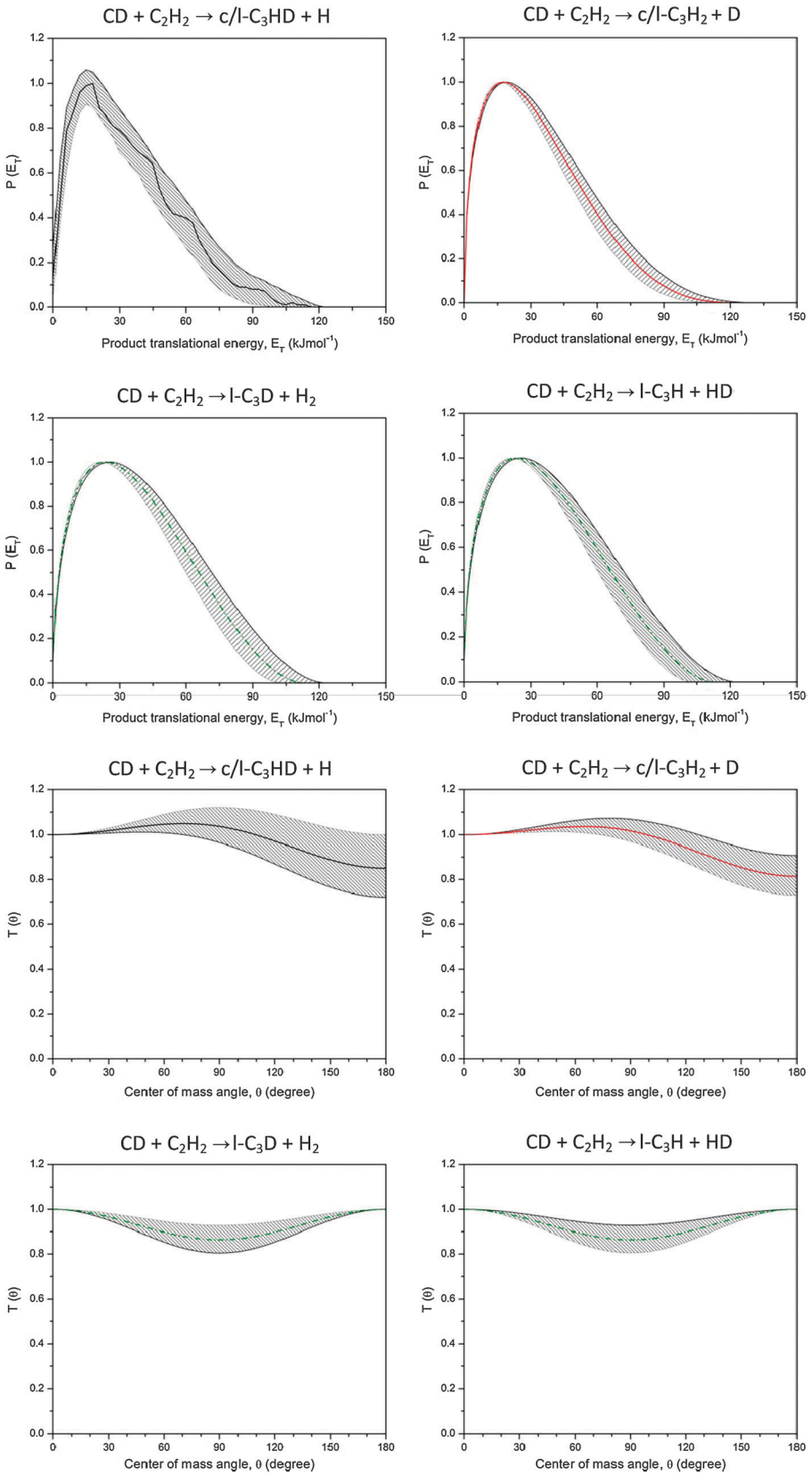

Fig. 5 Center-of-mass translational energy and angular distributions derived for the reaction channels in the D1-methylidyne–acetylene system.

longer than its rotational period. Further, the dip at 90° indicates geometrical constraints and a preferential loss of the H_2 and HD within the rotational plane of the decomposing complex(es) almost perpendicularly to the total angular momentum vector. It should be noted that the center-of-mass functions for channels (1c) and (1d) are basically the same to

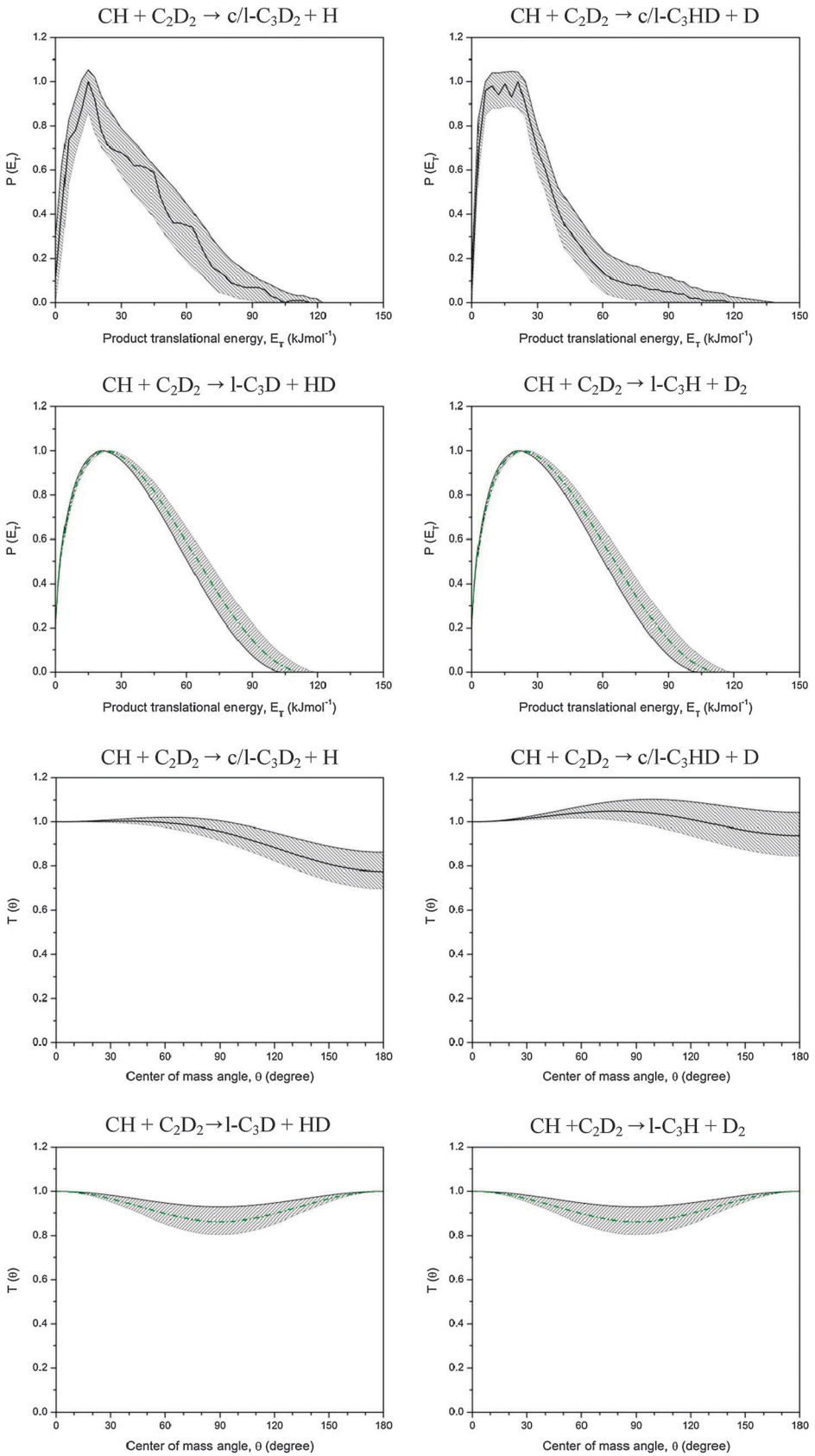

Fig. 6 Center-of-mass translational energy and angular distributions derived for the reaction channels in the methylidyne–D2-acetylene system.

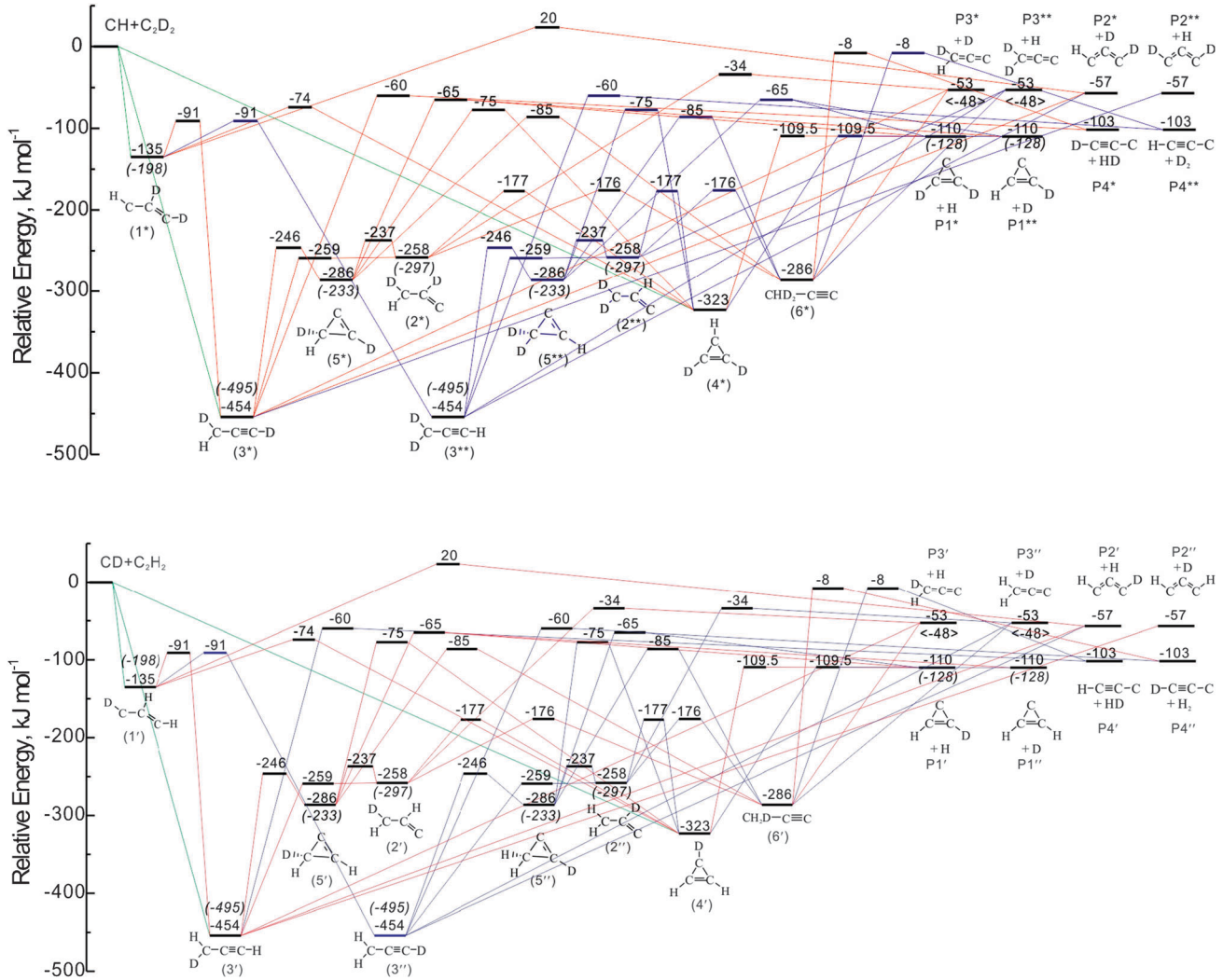

Fig. 7 Schematic potential energy surface of the reaction of methylidyne radicals with D2-acetylene (top) and for D1-methylidyne with acetylene compiled (bottom) from Mebel *et al.*, Goulay *et al.* (values in round brackets), and Vazquez *et al.* (values in angle brackets). Energies are given for the methylidyne–acetylene system; due to the differences in zero point energies, energies for the methylidyne–D2-acetylene and D1-methylidyne–acetylene systems differ by less than 10 kJ mol^{-1}.

those derived for the l-C_3H + H_2 channel for the reaction of methylidyne radicals with acetylene.[47]

4.2. CH/C_2D_2 System

Considering the center-of-mass functions for the methylidyne–D2-acetylene system, the functions for the C_3D_2 + H (2a) and C_3DH + D channels (2b) are within the error limits identical to those used to fit the data for the C_3DH + H and C_3H_2 + D pathways (channels (1a) and (1b)) in the D1-methylidyne–acetylene system (Fig. 6). Therefore, we can conclude that the reaction of methylidyne with D2-acetylene proceeds *via* C_3D_2H complex formation in an indirect fashion yielding—based on the derived energetics—*via* atomic hydrogen elimination at least the c-C_3D_2 and c-C_3DH isomers. Finally, let us turn our attention to the HD and D_2 elimination channels (2c) and (2d) leading to C_3D and C_3H, respectively. It strikes that the laboratory data were fit with identical center-of-mass functions for both channels, which are in turn close to those utilized to fit the data for the C_3D + H_2 and C_3H + HD channels in the D1-methylidyne plus acetylene reaction and also in the methylidyne–acetylene system.[47] The experimentally derived reaction energy of -93 ± 10 kJ mol^{-1} suggests the formation of l-C_3D + H_2 and l-C_3H + HD. Also, the forward–backward symmetry and intensity over the complete angular range indicate complex forming (indirect) scattering dynamics and a life time of the decomposing C_3D_2H complex longer than its rotational period. Further, the dip at 90 ° indicates geometrical constraints and a preferential loss of the D_2 and HD within the rotational plane of the decomposing complex(es) almost perpendicularly to the total angular momentum vector.

4.3. Proposed reaction dynamics

Before we propose the underlying reaction dynamics, it is advisable to summarize the results obtained so far.

R1: in the CD/C_2H_2 system, four channels (1a–1d) were identified. All pathways involved indirect scattering dynamics *via* C_3H_2D complex(es) formation.

R2: channels (1a) and (1b) lead *via* atomic hydrogen and deuterium elimination to at least c-C_3DH and c-C_3H_2 isomers, respectively. Based on the one-channel fits alone, contributions from CCCDH/HCCCD and $CCCH_2$/HCCCH cannot be ruled out.

R3: channels (1c) and (1d) undergo H_2 and HD elimination forming l-C_3D and l-C_3H, respectively. The molecular elimination channels exhibit geometrical constraints: the molecular H_2 and HD fragments are emitted within the plane of the rotating C_3H_2D complex.

R4: the atomic hydrogen/deuterium elimination pathways dominate the outcome of the reaction (81 ± 23%) compared to the molecular elimination pathways (19 ± 10%).

R5: in the CH/C_2D_2 system, four channels (2a–2d) were identified as well, all involving indirect scattering dynamics *via* C_3D_2H complex(es) formation.

R6: channels (2a) and (2b) lead *via* atomic hydrogen and deuterium elimination to at least the c-C_3D_2 and c-C_3DH isomers, respectively. Based on the one-channel fits alone, contributions from $CCCD_2$/DCCCD and CCCHD/HCCCD cannot be ruled out.

R7: channels (2c) and (2d) undergo HD and D_2 elimination forming l-C_3D and l-C_3H, respectively. Also, the molecular elimination channels depict geometrical constraints: the molecular D_2 and HD fragments are emitted within the plane of the rotating C_3D_2H complex.

R8: the atomic hydrogen/deuterium elimination pathways dominate the outcome of the reaction (87 ± 30%) compared to the molecular elimination pathways (13 ± 4%).

Molecular 'hydrogen' elimination. These results hold important conclusions to understand the underlying reaction dynamics. Let us first focus on the molecular 'hydrogen' elimination channels leading to l-C_3D + H_2 (1c) and l-C_3H + HD (1d) (CD/C_2H_2) as well as C_3D + HD (2c) and C_3H + D_2 (2d) (CH/C_2D_2). A look at the relevant potential energy surfaces (Fig. 7) reveals that only intermediates (3)/(6) can undergo this molecular hydrogen elimination pathway. Considering the CD/C_2H_2 system, the propargyl radical structures (3′) and (3″) can emit HD and H_2, respectively, whereas (6′) can lose HD and/or H_2 from the methyl group. For the CH/C_2D_2 system, (3*) and (3**) are able to eject HD and H_2, respectively; (6*) can lose HD and/or D_2. What might be the role of (6′)? This intermediate cannot be formed in one step pathway from the separated reactants, but must involve intermediates (2′)/(2″), (5′)/(5″) and/or the sequences (5′) → (2′) and/or (5″) → (2″). The isomerization of (5′) and (5″) to (6′) proceeds *via* a simultaneous hydrogen/deuterium-shift and ring opening over a significant barrier of 148–202 kJ mol^{-1}; on the other hand, (2′)/(2″) isomerize *via* barriers of 'only' 82–121 kJ mol^{-1}. Hence, if (6′) plays a role in the reaction dynamics, it is preferentially formed *via* isomerization of (2′)/(2″). The latter intermediates can be accessed *via* (3′)(3″), (4′)/(4″), and/or (5′)/(5″). Considering the isomerization barriers, (2′)/(2″) would rather rearrange to (5′)/(5″) over a relatively small barrier of only 21–60 kJ mol^{-1} than isomerizing to (6′) or (4′)/(4″). Therefore, we can conclude that if (2′)/(2″) is formed, the enhanced barrier to isomerization would prevent the formation of (6′). Hence, we suggest that the 'molecular' hydrogen elimination channels cannot be initiated by (6′). This leaves the propargyl radical intermediates (3′)/(3″) as the only viable reaction intermediate to open channels (1c) and (1d). The involvement of the propargyl intermediates (3′) and/or (3″) is worth mentioning. Note that an insertion process of the CD radical into the carbon–hydrogen bond of acetylene can only yield (3). On the other hand, an addition of CD to one of the acetylenic carbon atoms forms a weakly bound intermediate (1′), which can undergo a hydrogen shift from the central to the terminal carbon atoms holding a deuterium or hydrogen atom forming (3′) and (3″), respectively. Neither channel has any entrance barrier. Since both channels (1c) [from (3″)] and (1d) [from (3′)] have similar branching ratios, we might conclude that, under the absence of pronounced isotopic effects, (3′) and (3″) are formed in similar amounts. If the addition of CD forming (1′) largely dominates over the insertion to (3′), then the hydrogen shift in (1′) should form similar amounts of (3′) and (3″). This in turn is expected to result in similar branching ratios for the HD and H_2 elimination pathways. However, if the CD insertion is also present—which can only yield (3′), then (3′) should be formed preferentially compared to (3″). This in turn would suggest that the HD elimination from (3′) should have a larger branching ratio than the H_2 elimination from (3″). Also, a lack of any (3″) should be reflected in the absence of the H_2 elimination pathway, which was clearly not observed. Consequently, we can conclude that the experimentally observed H_2 elimination must be the result of the presence of (3″) formed *via* hydrogen shift in (1′), which in turn is accessed *via* the reactants by barrierless addition of the CD radical to one carbon atom of the acetylene molecule. Therefore, our experimental findings of the molecular 'hydrogen' elimination pathways suggest that the CD radical adds to the acetylenic carbon atom forming (1′) which in turn undergoes hydrogen shifts to (3′) and (3″). The H_2 elimination can proceed only from (3″), whereas HD can be only emitted from (3′). In the absence of any isotopic effects, both HD and H_2 should be formed in equal amounts. The slightly preferential formation of HD compared to H_2 *might* indicate an additional pathway forming (3′): the insertion of CD into the carbon–hydrogen bond of acetylene. In the CD/C_2H_2 system, the decomposition of propargyl intermediates (3*) and (3**) can lead to HD and D_2 loss, respectively. Here, channels C_3D + HD and C_3H + D_2 have similar branching ratios. This suggests that (3*) and (3**) might be formed in equal amounts and—in line with the previous discussion—most likely from (1*) *via* atomic deuterium shift. Note that if CH is also inserted into a C–D bond of D2-acetylene, (3*) should have higher concentrations than (3**). This should be reflected—in the absence of any isotopic effects—in an enhanced formation of HD compared to D_2. However, within the experimental error limits of the branching ratios, this has not been observed. The preferential addition of the methylidyne and D1-methylidyne radicals to the acetylene molecule compared to insertion into a carbon–hydrogen/deuterium bond can be rationalized in terms of the higher cone of acceptance of the carbon–carbon triple bond compared to the carbon–hydrogen/deuterium single bond.

Therefore, we might conclude that—if present—the insertion of the CD/CH radical into the carbon–hydrogen and carbon–deuterium bonds plays only a minor role; the dominant pathways

leading to the molecular 'hydrogen' loss involve an addition of CD/CH to the carbon atom of the acetylene/D2-acetylene molecule followed by hydrogen/deuterium shifts leading to (3′)/(3″) and (3*)/(3**) which in turn fragment *via* HD/H_2 and HD/D_2 elimination, respectively. It should be stressed that the observance of the D_2 and H_2 elimination can be only explained by the existence of (3**) and (3″), respectively, which in turn can be formed from (1*) and (1′) *via* deuterium and hydrogen shift, respectively. A look at the pertinent PES suggests that the molecular 'hydrogen' loss pathways involve tight exit transition states located about 43 kJ mol^{-1} above the energy of the separated reactants. The involvement of relatively tight exit transition states was predicted based on the center-of-mass translational energy distributions. Also, recall that computed geometries of the exit transition states involved in the molecular 'hydrogen' loss pathways[47] suggest that molecular hydrogen is ejected almost in the plane of the decomposing intermediate. Here, one hydrogen atom of the leaving molecular hydrogen was calculated to depart at an angle of about 1.1 ° below and the second hydrogen atom 7.4 ° above the molecular plane. This theoretical prediction is fully supported by our experimental finding of $T(\theta)$s for the HD, H_2, and D_2 elimination pathways holding a minimum at 90°, *i.e.* a preferential emission of molecular hydrogen within the plane of the decomposing complex. As discussed above, an alternative pathway connects intermediate CH_3CC (6) to l-C_3H plus molecular hydrogen. This mechanism was discounted for by the inspection of the relative barrier height of isomerization concluding that (6′) and (6*) play no role in the underlying reaction dynamics. This conclusion also gains support from the computed geometry of the transition state connecting intermediate (6) and l-C_3H/C_3D indicating that molecular 'hydrogen' is lost perpendicularly to the rotational plane at an angle of about 86.7°. This clearly contradicts our experimental finding. Therefore, we can dismiss that intermediate (6) plays a role in the chemical dynamics of this channel.

In conclusion, we can state that l-C_3H/C_3D plus molecular 'hydrogen' in the form of HD, H_2, and D_2 is formed *via* unimolecular decomposition of long lived propargyl radical intermediates (3′)/(3″)/(3*)/(3**) *via* rather tight exit transition states. The experimental observation of the H_2 and D_2 channels presents direct evidence of the existence of (3″) and of (3**), which in turn were formed *via* addition of CD and CH to the carbon atom of acetylene/D2-acetylene followed by isomerization of (1′) and (1*), respectively. This isomerization can also lead to (3′) and (3*), which then each generate the HD product. Finally, our experimental results do not provide evidence of a dominant insertion of CH or CD into the acetylenic carbon–deuterium or carbon–hydrogen bond.

Atomic 'hydrogen' elimination. The energetics derived from the center-of-mass translational energy distributions for the atomic hydrogen and deuterium elimination pathways (1a), (1b), (2a), and (2b) suggest that at least the energetically favorable cyclic structures, c-C_3DH, c-C_3D_2, and c-C_3H_2, are formed. The essentially identical center-of-mass angular distributions might suggest that the dynamics to form these species are similar and involve indirect scattering dynamics *via* C_3D_2H and C_3H_2D intermediates, respectively. Based on the potential energy surfaces, the cyclic products can be formed *via* decomposition of (4′) and (4*) or (5′)/(5″) or (5*) or (5**). (5)/(5″) and (4′) as well as (5*)/(5**) and (4*) are connected *via* hydrogen/deuterium shifts *via* significant barriers of about 158–221 kJ mol^{-1}. However, the PESs suggest that based on the inherent barriers, the isotopologues/isotopomers of (5) rather isomerize to isotopologues/isotopomers of (2) and (3); the barriers involved in these processes are at least 100 kJ mol^{-1} lower than the competing hydrogen/deuterium shifts to (4′)/(4*). Once formed from addition of CD and CH to the acetylenic carbon–carbon triple bond of acetylene and D2-acetylene, (4′) and (4*) can decompose *via* atomic hydrogen and deuterium loss, respectively. It should be noted that in (4′), the CD unit is added 'on top' of the acetylene molecule. Since (4′) was found to decompose *via* atomic hydrogen and deuterium loss, the energy randomization might be complete thus allowing energy to 'flow' from the initially formed carbon–carbon bonds to the carbon–hydrogen and carbon–deuterium bonds in order to eject in competing channels a hydrogen atom and a deuterium atom. This situation is similar for the intermediate (4*) formed *via* addition of methylidyne and D2-acetylene. The likely energy randomization and redistribution from the initially formed carbon–carbon bonds allows an atomic deuterium and hydrogen loss.

Having established that the fragmentation of propargyl radical isotopologues/isotopomers (3′)/(3″)/(3*)/(3**), leads to molecular 'hydrogen' elimination (HD, H_2, D_2) and that a unimolecular decomposition of cyclopropenyl radicals (4′)/(4**) results in atomic hydrogen and deuterium loss, we are finally turning our attention to the possible role of two alternative product molecules: isotopologues/isotopomers of propargylene and vinylidene carbene (P2 and P3, respectively). It should be stressed that based on the single channel fit center-of-mass translational energy distributions alone, the present experiments can say nothing about the possible participation of propargylene or vinylidene carbene. However, a previous study on the methylidyne–acetylene system suggested that the single center-of-mass translational energy distribution could be split up into two contributions accounting for c-C_3H_2 and HCCCH/H_2CCC.[47] Considering the energetics and barriers involved in the decomposition of the propargyl radicals, the PESs suggest that propargyl should also decompose to propargylene/vinylidene carbene. Note that each of the (3′)/(3″)/(3*)/(3**) intermediates could lose atomic and/or molecular hydrogen. Therefore, the experiments within the CD/C_2H_2 and CH/C_2D_2 systems do not provide direct evidence of the involvement of propargylene/vinylidene carbene, but only indirectly based on PESs and the energetics together with the heights of the barriers involved. However, since the center-of-mass translational energy distributions are essentially identical to those derived from the CH/C_2H_2 system, where we could split up the single channel fit for the atomic hydrogen loss pathway into two components with the constraints as discussed in reference,[47] even the present experimental data might indirectly suggest the formation of propargylene/vinylidene carbene. Considering the molecular formulae of the reaction intermediates formed in the CH/D2–acetylene and CD/acetylene systems, *i.e.* C_3D_2H and C_3H_2D, we should see an enhanced deuterium loss from the decomposition of C_3D_2H intermediates, but an enhanced hydrogen loss from C_3H_2D intermediates. The derived branching ratios show this tendency and reflect a

preferential hydrogen loss from C_3H_2D [50 ± 15% *vs.* 31 ± 8%] and enhanced deuterium loss from C_3D_2H intermediates [34 ± 15% *vs.* 53 ± 15%].

5. Summary and conclusion

We conducted the crossed molecular beam reactions of ground state methylidyne radicals, $CH(X^2\Pi)$, with D2-acetylene, $C_2D_2(X^1\Sigma_g^+)$, and of D1-methylidyne radicals, $CD(X^2\Pi)$, with acetylene, $C_2H_2(X^1\Sigma_g^+)$, at a collision energy of 17 kJ mol^{-1} under single collision conditions. We propose that the reaction dynamics of the methylidyne/D1-methylidyne radical with D2-acetylene/acetylene are indirect *via* complex formation and are initiated by a barrierless addition to one and to both carbon atoms of the acetylene reactant yielding intermediates (1′)/(1*) and (4′)/(4*), respectively. Based on the experimentally derived branching ratios of the H_2 *vs.* HD and HD *vs.* D_2 molecular 'hydrogen' elimination pathways, an insertion of the CH/CD into the carbon–deuterium/carbon–hydrogen bond of the acetylene molecule can be likely ruled out. This result agrees well with previous kinetics studies of these systems by Taatjes *et al.*[62] at temperatures between 291 and 710 K suggesting that addition dominated the association. As evident from the branching ratios of the atomic hydrogen/deuterium loss channels, the cyclopropenyl radical (4′)(4*) holds a lifetime sufficient enough to channel the energy from the initially formed carbon–carbon bonds to the carbon–hydrogen and carbon–deuterium bonds thus undergoing unimolecular decomposition by the emission of atomic hydrogen and atomic deuterium leading to cyclopropenylidene (c-C_3H_2, c-C_3D_2, c-C_3DH). On the other hand, adduct (1′)/(1*) undergoes hydrogen/deuterium shifts to a long lived propargyl radical ((3′)/(3″)/(4*)/(4**)); the latter decomposes *via* molecular 'hydrogen' loss within the rotational plane of the decomposing complex to l-C_3H/l-C_3D. Considering the barriers involved in the competing unimolecular decomposition pathways of the propargyl radical, *i.e.* an atomic *versus* molecular 'hydrogen' elimination', the formation of the thermodynamically less stable isotopomers of propargylene (P2) and/or vinylidene carbene (P3) is also likely. A comparison of the branching ratios from the previous experiments under single collision conditions with those derived from our previous study on the methylidyne–acetylene system[47] supports the trend of a dominating atomic 'hydrogen' loss. Here, branching ratios for the atomic *versus* molecular hydrogen loss pathways were derived to be 91 ± 10% and 9 ± 2%, respectively, for the methylidyne–acetylene reaction. The tendency of a dominant atomic 'hydrogen' loss is also observed in the present studies: 81 ± 23% *vs.* 19 ± 10% for the CD/C_2H_2 and 87 ± 30% *vs.* 13 ± 4% for the CH/C_2D_2 systems.

The dominance of the atomic 'hydrogen' loss pathway has also important astrochemical implications. Two C_3H_2 isomers, *i.e.* cyclopropenylidene (c-C_3H_2) and vinylidene carbene (H_2CCC), have been identified in the interstellar medium. In a pioneering study, Thaddeus *et al.* observed twenty seven rotational lines of *ortho* c-C_3H_2[85] such as in the Taurus Molecular Cloud (TMC-1) as well as toward Orion KL, Sagittarius B2, and planetary nebulae like NGC 7293.[86] The thermodynamically less stable vinylidene carbene (H_2CCC) isomer, which has been considered recently as a candidate for the broad, diffuse interstellar bands (DIBs) at 4881 and 5450 Å,[87] was detected in TMC-1 with fractional abundances of only about 1% of the cyclic isomer.[88] The singly deuterated c-C_3HD, detected toward L 1498 and TMC-1, depicts unique deuterium enrichment with a ratio of fractions of [c-C_3HD]/[c-C_3H_2] ~0.05–0.15.[89] Our studies provide therefore evidence that the reaction of methylidyne radicals with acetylene and possibly with D1-acetylene or of D1-methylidyne with acetylene can lead at least to the c-C_3HD and c-C_3H_2 species under single collision conditions *via* a single, barrier-less and exoergic encounter of two neutral reactants. On the other hand, the branching ratios of the 'molecular' hydrogen loss channel in the order of 10% at most suggest that the l-C_3H radical, as observed toward TMC-1,[90] is unlikely to be formed in the methylidyne–acetylene system in sufficient concentrations to account for the astronomical observations. Note that no synthetic route to the ubiquitous c-C_3H monitored in TMC-1[91] exists in the reaction of methylidyne with acetylene. However, as shown previously, both the cyclic and linear C_3H isomers can be easily formed *via* the neutral–neutral reaction of ground state carbon atoms with acetylene in a single collision event.[41,92–99]

Acknowledgements

This project was supported by the US National Science Foundation (NSF-0948258) and by the US Department of Energy Office of Science (DE-FG02-03-ER15411). We thank Professor Alexander M. Mebel (Florida International University) for discussions.

References

1 D. Calzetti, *EAS Publ. Ser.*, 2011, **46**, 133–141.
2 I. Cherchneff, *EAS Publ. Ser.*, 2011, **46**, 177–189.
3 Combustion Chemistry: Elementary Reactions to Macroscopic Processes, *Faraday Discuss.*, 2001, **119**.
4 J. Appel, H. Bockhorn and M. Frenklach, *Combust. Flame*, 2000, **121**, 122–136.
5 C. E. Baukal, *Oxygen Enhanced Combustion*, 1998.
6 M. F. Budyka, T. S. Zyubina, A. G. Ryabenko, V. E. Muradyan, S. E. Esipov and N. I. Cherepanova, *Chem. Phys. Lett.*, 2002, **354**, 93–99.
7 F. Cataldo and Editor, *Polyynes: Synthesis, Properties, and Applications*. (*Interdisciplinary Meeting on Polyynes and Carbyne held 30–31 October 2003 in Naples, Italy.*), 2006.
8 M. Frenklach, *Phys. Chem. Chem. Phys.*, 2002, **4**, 2028–2037.
9 A. Kazakov and M. Frenklach, *Combust. Flame*, 1998, **112**, 270–274.
10 A. Kazakov and M. Frenklach, *Combust. Flame*, 1998, **114**, 484–501.
11 Y.-T. Lin, R. K. Mishra and S.-L. Lee, *J. Phys. Chem. B*, 1999, **103**, 3151–3155.
12 A. Necula and L. T. Scott, *J. Am. Chem. Soc.*, 2000, **122**, 1548–1549.
13 A. M. Nienow and J. T. Roberts, *Annu. Rev. Phys. Chem.*, 2006, **57**, 105–128.
14 H. Richter and J. B. Howard, *Prog. Energy Combust. Sci.*, 2000, **26**, 565–608.
15 L. Vereecken, H. F. Bettinger and J. Peeters, *Phys. Chem. Chem. Phys.*, 2002, **4**, 2019–2027.
16 A. Soewono and S. Rogak, *Aerosol Sci. Technol.*, 2011, **45**, 1206–1216.
17 S. Zhang, Q. He, R. Li, Q. Wang, Z. Hu, X. Liu and X. Chang, *Mater. Lett.*, 2011, **65**, 2371–2373.
18 C. C. Austin, D. Wang, D. J. Ecobichon and G. Dussault, *J. Toxicol. Environ. Health*, 2001, **63**, 437–458.

19 A. Ergut, Y. A. Levendis, H. Richter and J. Carlson, *Fourth Jt. Meet. U.S. Sect. Combust. Inst.: West. States, Cent. States, East. States*, 2005, pp. A05/01–A05/06.
20 D. B. Atkinson and J. W. Hudgens, *J. Phys. Chem. A*, 1999, **103**, 4242–4252.
21 D. K. Hahn, S. J. Klippenstein and J. A. Miller, *Faraday Discuss.*, 2001, **119**, 79–100.
22 D. J. Mann and W. L. Hase, *J. Am. Chem. Soc.*, 2002, **124**, 3208–3209.
23 H. Guo and G. J. Smallwood, *Combust. Theory Modell.*, 2011, **15**, 125–140.
24 S. A. Skeen, G. Yablonsky and R. L. Axelbaum, *Chem. Phys. Processes Combust.*, 2009, skeen2/1–skeen2/9.
25 C. F. Melius, J. A. Miller and E. M. Evleth, *Symp. (Int.) Combust., [Proc.]*, 1992, **24**, 621–628.
26 J. A. Miller and S. J. Klippenstein, *J. Phys. Chem. A*, 2003, **107**, 7783–7799.
27 Y. Georgievskii, J. A. Miller and S. J. Klippenstein, *Phys. Chem. Chem. Phys.*, 2007, **9**, 4259–4268.
28 L. B. Harding, S. J. Klippenstein and J. A. Miller, *J. Phys. Chem. A*, 2008, **112**, 522–532.
29 R. D. Kern and K. Xie, *Prog. Energy Combust. Sci.*, 1991, **17**, 191–210.
30 J. A. Miller and C. F. Melius, *Combust. Flame*, 1992, **91**, 21–39.
31 J. A. Miller, M. J. Pilling and J. Troe, *Proc. Combust. Inst.*, 2005, **30**, 43–88.
32 J. A. Miller, J. P. Senosiain, S. J. Klippenstein and Y. Georgievskii, *J. Phys. Chem. A*, 2008, **112**, 9429–9438.
33 J. P. Senosiain, S. J. Klippenstein and J. A. Miller, *Proc. Combust. Inst.*, 2007, **31**, 185–192.
34 N. Balucani, G. Capozza, F. Leonori, E. Segoloni and P. Casavecchia, *Int. Rev. Phys. Chem.*, 2006, **25**, 109–163.
35 E. Buonomo and D. C. Clary, *J. Phys. Chem. A*, 2001, **105**, 2694–2707.
36 D. C. Clary, E. Buonomo, I. R. Sims, I. W. M. Smith, W. D. Geppert, C. Naulin, M. Costes, L. Cartechini and P. Casavecchia, *J. Phys. Chem. A*, 2002, **106**, 5541–5552.
37 M. Frenklach and E. D. Feigelson, *Astrophys. J.*, 1989, **341**, 372–384.
38 X. Gu, Y. Guo, F. Zhang and R. I. Kaiser, *J. Phys. Chem. A*, 2007, **111**, 2980–2992.
39 E. Ionescu and S. A. Reid, *J. Mol. Struct. (THEOCHEM)*, 2005, **725**, 45–53.
40 W. M. Jackson, D. S. Anex, R. E. Continetti, B. A. Balko and Y. T. Lee, *J. Chem. Phys.*, 1991, **95**, 7327–7336.
41 R. I. Kaiser, C. Oschsenfeld, M. Head-Gordon, Y. T. Lee and A. G. Suits, *Science*, 1996, **274**, 1508–1511.
42 A. M. Mebel, *Rev. Mod. Quantum Chem.*, 2002, **1**, 340–358.
43 A. M. Mebel, W. M. Jackson, A. H. H. Chang and S. H. Lin, *J. Am. Chem. Soc.*, 1998, **120**, 5751–5763.
44 J. A. Miller and S. J. Klippenstein, *J. Phys. Chem. A*, 2001, **105**, 7254–7266.
45 C. Ochsenfeld, R. I. Kaiser, Y. T. Lee, A. G. Suits and M. Head-Gordon, *J. Chem. Phys.*, 1997, **106**, 4141–4151.
46 W. K. Park, J. Park, S. C. Park, B. J. Braams, C. Chen and J. M. Bowman, *J. Chem. Phys.*, 2006, **125**, 081101.
47 P. Maksyutenko, F. Zhang, X. Gu and R. I. Kaiser, *Phys. Chem. Chem. Phys.*, 2011, **13**, 240–252.
48 J. A. Miller and S. J. Klippenstein, *J. Phys. Chem. A*, 2003, **107**, 2680–2692.
49 J. Aguilera-Iparraguirre, A. D. Boese, W. Klopper and B. Ruscic, *Chem. Phys.*, 2008, **346**, 56–68.
50 A. Bergeat, T. Calvo, F. Caralp, J.-H. Fillion, G. Dorthe and J.-C. Loison, *Faraday Discuss.*, 2001, **119**, 67–77.
51 I. Fernandez and G. Frenking, *Faraday Discuss.*, 2007, **135**, 403–421.
52 M. Hausmann and K. H. Homann, *Ber. Bunsen-Ges.*, 1997, **101**, 651–667.
53 G. Maier, H. P. Reisenauer, W. Schwab, P. Carsky, B. A. Hess, Jr. and L. J. Schaad, *J. Am. Chem. Soc.*, 1987, **109**, 5183–5188.
54 J. A. Miller, J. V. Volponi and J.-F. Pauwels, *Combust. Flame*, 1996, **105**, 451–461.
55 A. Mohajeri and M. J. Jenabi, *J. Mol. Struct. (THEOCHEM)*, 2007, **820**, 65–73.
56 H. P. Reisenauer, G. Maier, A. Riemann and R. W. Hoffman, *Angew. Chem.*, 1984, **96**, 596.
57 H. Richter and J. B. Howard, *Phys. Chem. Chem. Phys.*, 2002, **4**, 2038–2055.
58 R. A. Seburg, J. T. DePinto, E. V. Patterson and R. J. McMahon, *J. Am. Chem. Soc.*, 1995, **117**, 835–836.
59 R. A. Seburg, E. V. Patterson and R. J. McMahon, *J. Am. Chem. Soc.*, 2009, **131**, 9442–9455.
60 R. A. Seburg, E. V. Patterson, J. F. Stanton and R. J. McMahon, *J. Am. Chem. Soc.*, 1997, **119**, 5847–5856.
61 L. B. Harding, S. J. Klippenstein and Y. Georgievskii, *J. Phys. Chem. A*, 2007, **111**, 3789–3801.
62 C. A. Taatjes, S. J. Klippenstein, N. Hansen, J. A. Miller, T. A. Cool, J. Wang, M. E. Law and P. R. Westmoreland, *Phys. Chem. Chem. Phys.*, 2005, **7**, 806–813.
63 A. Bhargava and P. R. Westmoreland, *Combust. Flame*, 1998, **113**, 333–347.
64 J. D. Bittner, MIT, 1981.
65 G. E. Oulundsen, Univ. Massachussets, 1999.
66 P. R. Westmoreland, J. B. Howard, J. P. Longwell and A. M. Dean, *AIChE J.*, 1986, **32**, 1971–1979.
67 A. Canosa, I. R. Sims, D. Travers, I. W. M. Smith and B. R. Rowe, *Astron. Astrophys.*, 1997, **323**, 644–651.
68 J.-C. Loison and A. Bergeat, *Phys. Chem. Chem. Phys.*, 2009, **11**, 655–664.
69 H.-J. Deyerl, I. Fischer and P. Chen, *J. Chem. Phys.*, 1999, **111**, 3441–3448.
70 L. R. McCunn, B. L. FitzPatrick, M. J. Krisch, L. J. Butler, C.-W. Liang and J. J. Lin, *J. Chem. Phys.*, 2006, **125**, 133306.
71 S. J. Goncher, D. T. Moore, N. E. Sveum and D. M. Neumark, *J. Chem. Phys.*, 2008, **128**, 114303.
72 T. L. Nguyen, A. M. Mebel, S. H. Lin and R. I. Kaiser, *J. Phys. Chem. A*, 2001, **105**, 11549–11559.
73 A compilation of rate constants is given in http://kinetics.nist.gov/kinetics/index.jsp.
74 H. Thiesemann, J. MacNamara and C. A. Taatjes, *J. Phys. Chem. A*, 1997, **101**, 1881–1886.
75 W. Boullart, K. Devriendt, R. Borms and J. Peeters, *J. Phys. Chem.*, 1996, **100**, 998–1007.
76 K. McKee, M. A. Blitz, K. J. Hughes, M. J. Pilling, H.-B. Qian, A. Taylor and P. W. Seakins, *J. Phys. Chem. A*, 2003, **107**, 5710–5716.
77 F. Goulay, A. J. Trevitt, G. Meloni, T. M. Selby, D. L. Osborn, C. A. Taatjes, L. Vereecken and S. R. Leone, *J. Am. Chem. Soc.*, 2009, **131**, 993–1005.
78 X. Gu, Y. Guo, H. Chan, E. Kawamura and R. I. Kaiser, *Rev. Sci. Instrum.*, 2005, **76**, 116103.
79 X. Gu, Y. Guo, E. Kawamura and R. I. Kaiser, *Rev. Sci. Instrum.*, 2005, **76**, 083115/083111–083115/083116.
80 Y. Guo, X. Gu, E. Kawamura and R. I. Kaiser, *Rev. Sci. Instrum.*, 2006, **77**, 034701/034701–034701/034709.
81 Y. Guo, X. Gu and R. I. Kaiser, *Int. J. Mass Spectrom.*, 2006, **249/250**, 420–425.
82 R. I. Kaiser, P. Maksyutenko, C. Ennis, F. Zhang, X. Gu, S. P. Krishtal, A. M. Mebel, O. Kostko and M. Ahmed, *Faraday Discuss.*, 2010, **147**, 429–478.
83 M. Vernon, *PhD thesis*, University of California, Berkeley, 1981.
84 P. S. Weiss, *PhD thesis*, University of California, Berkeley, 1986.
85 P. Thaddeus, J. M. Vrtilek and C. A. Gottlieb, *Astrophys. J.*, 1985, **299**, L63–L66.
86 E. D. Tenenbaum, S. N. Milam, N. J. Woolf and L. M. Ziurys, *Astrophys. J.*, 2009, **704**, L108–L112.
87 J. P. Maier, G. A. H. Walker, D. A. Bohlender, F. J. Mazzotti, R. Raghunandan, J. Fulara, I. Garkusha and A. Nagy, *Astrophys. J.*, 2011, **726**, 41/1–41/9.
88 J. Cernicharo, C. A. Gottlieb, M. Guelin, T. C. Killian, G. Paubert, P. Thaddeus and J. M. Vrtilek, *Astrophys. J.*, 1991, **368**, L39–L41.
89 M. B. Bell, L. W. Avery, H. E. Matthews, P. A. Feldman, J. K. Watson, S. C. Madden and W. M. Irvine, *Astrophys. J.*, 1988, **326**, 924–930.
90 P. Thaddeus, C. A. Gottlieb, A. Hjalmarson, L. E. B. Johansson, W. M. Irvine, P. Friberg and R. A. Linke, *Astrophys. J.*, 1985, **294**, L49–L53.
91 J. G. Mangum and A. Wootten, *Astron. Astrophys.*, 1990, **239**, 319–325.

92 X. Gu, Y. Guo, F. Zhang and R. I. Kaiser, *J. Phys. Chem. A*, 2007, **111**, 2980–2992.
93 M. Costes, N. Daugey, C. Naulin, A. Bergeat, F. Leonori, E. Segoloni, R. Petrucci, N. Balucani and P. Casavecchia, *Faraday Discuss.*, 2006, **133**, 157–176.
94 M. B. Bell, L. W. Avery, H. E. Matthews, P. A. Feldman, J. K. G. Watson, S. C. Madden and W. M. Irvine, *Astrophys. J.*, 1988, **326**, 924–930.
95 E. D. Tenenbaum, S. N. Milam, N. J. Woolf and L. M. Ziurys, *Astrophys. J.*, 2009, **704**, L108–L112.
96 J. P. Maier, G. A. H. Walker, D. A. Bohlender, F. J. Mazzotti, R. Raghunandan, J. Fulara, I. Garkusha and A. Nagy, *Astrophys. J.*, 2011, **726**, 41/41–41/49.
97 J. Cernicharo, C. A. Gottlieb, M. Guelin, T. C. Killian, G. Paubert, P. Thaddeus and J. M. Vrtilek, *Astrophys. J.*, 1991, **368**, L39–L41.
98 P. Thaddeus, J. M. Vrtilek and C. A. Gottlieb, *Astrophys. J.*, 1985, **299**, L63–L66.
99 J. Vazquez, M. E. Harding, J. Gauss and J. F. Stanton, *J. Phys. Chem. A*, 2009, **113**, 12447–12453.

